Applied Physics A (2018) 124:491
https://doi.org/10.1007/s00339-018-1901-1

Applied Physics A
Materials Science & Processing

Reinforcement of polyaniline and poly-(o-toluidine) with SWNTs and tuning of their physicochemical properties by heavy ion beams

Harshada K. Patil[1] · Megha A. Deshmukh[1] · Gajanan A. Bodkhe[1] · Sumedh M. Shirsat[2] · K. Asokan[3] · Mahendra D. Shirsat[1]

Received: 27 February 2018 / Accepted: 7 June 2018

Abstract
In the present investigation, the organic conducting polymers (OCP) were reinforced with single-walled carbon nanotubes (SWNTs) through non-covalent interaction. The polyaniline/SWNTs and poly-(o-toluidine)/SWNTs composites were synthesized electrochemically, and the effects of the Swift heavy ions (SHI) irradiation of 100 MeV oxygen ions beam and 55 MeV carbon ions beam at various ion fluences were investigated, respectively. The spectroscopic and morphological studies were carried out using ultraviolet–visible spectroscopy, Fourier transformed infrared spectroscopy, Raman spectroscopy, and field-emission scanning electron microscopy respectively. Attempts have been made to reveal the influence of high-energy ion irradiation on composites which are highly sensitive and possess characteristics role in tuning of various properties. The facile approach indicates that the SHI irradiation can be adopted to enhance various functionalities of the OCPs reinforced with the SWNTs.

1 Introduction

The reinforcement of organic conducting polymers (OCP) matrix by nanostructured materials has been explored due to their potential applications in organic devices [1–5]. These OCPs have many applications due to their tuning of electrical conductivity ranging from semiconducting to metallic regimes respectively, which is closely related to the charge transfer rate and electrochemical redox efficiency [6]. There are enormous applications of OCPs in the field of chemical sensors, since these are sensitive for small perturbations and have potential to exhibit improved response. As a matter of fact in the field of sensors, the inculcation of improved sensitivity, selectivity, response time, etc. are necessarily important parameters. Nanostructured form of OCPs provides the feature of high surface-to-volume ratio and small dimensions, which are very beneficial for sensor applications. The enhanced interaction between the materials and analytes enhances with high surface area which leads to high sensitivity. The smaller dimensions enable fast adsorption/desorption kinetics for analytes and ultimately result into quick response time [7–10]. The composites of various types of OCPs with different nanostructured carbon nanomaterials such as graphene, carbon nanotubes, and carbon nanofibers have proved to be the most promising than that of the individually stands. The higher surface area of the nanostructured carbon nanomaterial facilitated the higher surface area for the deposition of OCPs providing the efficient ion diffusion phenomenon facilitating the improved electrochemical responses [11–14].

The electronic structure which is determined by the chain symmetry of the OCPs possesses the characteristic property to tune the conductivity from semiconducting to metallic regime. The intrinsic conductivity results from the formation of charge carriers upon oxidizing (p-doping) or reducing (n-doping) their conjugated backbone which can be enabled through the interaction of analyte. This flexibility in modulation of OCPs allowed the applicability in various fields especially in chemical sensors [6]. However, inculcation of the SWNTs to the polymer matrix enables the excellent transduction [16] to the sensor platform, and therefore, the

✉ Mahendra D. Shirsat
mdshirsat.phy@bamu.ac.in

[1] Department of Physics, Centre for Advanced Sensor Technology, RUSA, Dr. Babasaheb Ambedkar Marathwada University, Aurangabad, Maharashtra 431 004, India

[2] Jawaharlal Nehru Engineering College, Aurangabad, Maharashtra 431 003, India

[3] Inter University Accelerator Centre, Aruna Asaf Ali Marg, New Delhi 110067, India

Published online: 14 June 2018

composites of both OCPs and SWNTs favour the characteristic features to the sensors.

Swift heavy ion (SHI) irradiation is one of the experimental tools mostly used for the modification of materials. The SHI irradiation, in case of OCPs, plays very crucial role in tuning various factors such as crosslinking, creation of defect sites in molecular structure, structural rearrangements, molecular emission, etc. The change induced by SHI irradiation in morphological and electrical properties of the material provides aptitude to approach enormous applications of the material [15–17]. Therefore, SHI irradiation is well agreement in tuning the physicochemical properties of the materials. When the energetic ions interact/pass through the atoms of materials, there is loss of energy in two processes: one belongs to nuclear energy loss S_n and another electronic energy loss S_e. The energy lost through elastic collisions which is dominant at low energies is nuclear energy loss S_n, and energy lost through inelastic collusions which is dominant at high energies (> 1 MeV/nucleon) is electronic energy loss S_e. As energy is lost in inelastic collusions, while interaction with the atoms leads to excitation or ionization of the atoms [18], and ultimately results into significant modifications into the material. There are some reports in the literature, wherein the researchers have reported the effects of SHI irradiation with different ions with different energies and fluences on conducting polymers; A M P Hussain et al. have reported the 160 MeV Ni^{12+} ion irradiation on HCl-doped polyaniline electrode [15, 19] and polypyrrole electrode materials [20]. In these reports, authors have investigated the properties such as dc conductivity, degree of crystallinity, electrochemical stability, etc. They have observed improvement in the properties due to the deposition of huge amounts of energy due to the electronic energy loss by the incident high-energy ion during irradiation, which creates ions, radicals, and charged species. Effect of 100 MeV Ag^{8+} ions irradiation on polypyrrole has also been investigated through electrical and morphological characteristics, and appealed the scope for the applicability of irradiated conducting polymers as microstructures with defined conductivity for sensor applications [21].

Moreover, the materials with improved characteristic features are also explored enormously for the development of efficient devices. Preparation of hybrid materials/composites is an interesting approach to enhance the desired properties. Nanocomposites of OCPs with carbon nanotubes (CNTs) were first reported by Ajayan et al. in 1994. Carbon nanotubes provides themselves as best materials in reinforcing materials, since it possess smaller size, i.e., having molecular dimensions, and consist of perfect graphite sheets rolled into hollow cylinders. The carbon atoms present in CNTs are arranged in cylindrical hexagonal honeycomb lattices, and therefore ultimately possess unique electronic and transport properties [22]. Chuang Peng et al. have reported that electrochemical deposition of the composite gives the most homogeneous and shows an unusual interaction between the polymer and nanotubes which emphasizes electron delocalization and conjugation along the polymer chains [13]. Therefore, in chemical sensors, OCPs have been used as selective layers [5] and CNTs as conduction backbones [23–25]. In the family of polyaniline (PANI), with ring-substitution derivatives are been derived and studied for various applications, poly-o- toluidine (PoT) is one of the derivatives having methyl group at ortho-position possess faster switching time between the reduced and oxidized states [26–28]. In the present investigation, PANI and PoT were reinforced with SWNTs and these electrochemically synthesized composites were explored for SHI irradiation. The objective of this investigation is to evaluate the influence of irradiation in tuning the spectroscopic and morphological properties of both the composites at different ion fluences.

2 Experimental details

2.1 Materials and methods

For the synthesis of composite, monomers aniline and o-toluidine were purchased of reagent grade (purchased from Molychem) and were distilled prior to use. Sulphuric acid (H_2SO_4—purchased from Molychem) was used as dopant in preparation of electrolyte for both the composites. COOH-functionalised SWNTs were purchased from Nanoshel LLC-Wilmington, DE, USA. The composite of conducting polymers (CP), viz., PANI, and PoT with SWNTs were synthesized using electrochemical cyclic voltammetry technique. The electrochemical cell used was the conventional single-cell compartment assembly consisting of three electrodes. Indium tin oxide (ITO)-coated glass–planar substrate is used as working electrode, platinum as counter, and saturated Ag/AgCl as reference electrode. The synthesis of composite was performed at normal room temperature.

2.2 Instruments

CH Instruments CH660C electrochemical workstation was used for electrochemical synthesis of composites. The 15UD palletron facility available at Inter University Accelerator Centre, New Delhi (India) was used for SHI irradiation. UV–Vis spectra were recorded using Hitachi U-3300 spectrophotometer. FT-IR absorption spectra were obtained from Bruker Alpha Model. Raman spectra were obtained by Seki Technotonics of make STR 150 Raman spectrometer. FESEM images were recorded by TESCAN, MIRA II LMH CS.

2.3 Preparation of composites

In the electrochemical synthesis of both composites, sulphuric acid (H_2SO_4) was used as dopant with 0.2 M concentration. The monomer concentration of aniline and o-toluidine was kept 0.1 M, and SWNTs were taken equal to 10 weight percent (10 wt%) with respect to concentration of each monomers. Suspension of SWNTs was prepared in distilled water. The ratio of SWNTs and dodecyl-benzene-sulphonic acid (DBSA—used as surfactant) was equal to 1:10.

2.4 SHI irradiation

Composites of PANI/SWNTs and PoT/SWNTs were exposed to various ion fluences, viz., 5×10^{10}, 1×10^{11}, 5×10^{11}, and 1×10^{12} ions/cm^2 of 100 MeV oxygen ion beam (charge state +7 and beam current 0.5 pnA) and 55 MeV carbon ion (with the charge state +6 and beam current 0.5 pnA), respectively.

2.5 SRIM calculations

SRIM (Stopping and Range of Ions in Matter, version 2008.04) program was used for determination of electronic and nuclear energy loss occurring during interaction of high-energy ion beam, viz., oxygen ion and carbon ion interacting with PANI/SWNTs composite and PoT/SWNTs composite, respectively.

3 Results and discussion

3.1 Electrochemical synthesis

Figure 1 shows the electrochemical synthesis of PANI/SWNTs and PoT/SWNTs composites using cyclic voltammetry technique. The electrochemical deposition of both the composites was carried out on ITO glass electrode (having geometrical area of 1 cm^2). The dynamic potential window for PANI/SWNTs was kept 0.1 to 1.0 V (number of cycles 15) and 0.1–1.2 V (number of cycles 30) for PoT/SWNTs with respective scan rate equal to 0.1 V/s. During synthesis process, it was observed for both composites that there is an increase in current with stepping to next cycle indicating the formation of composite and electroactive nature of the electrode. The PANI/SWNTs composite shows oxidation peaks at 0.3 and 0.6 V, and reduction peak at 0.45 V respectively. The PoT/SWNTs composite shows oxidation peak at 0.9 and 4.5 V, and reduction peak at 0.65 V, respectively. The reduction/oxidation peak indicates the growth mechanism of the OCPs, and it depends on the anions present in the electrolyte [29]. Formation of composite involves the interaction between π–π^* electrons between monomers and SWNTs also the hydrogen bonding interaction of carboxyl groups

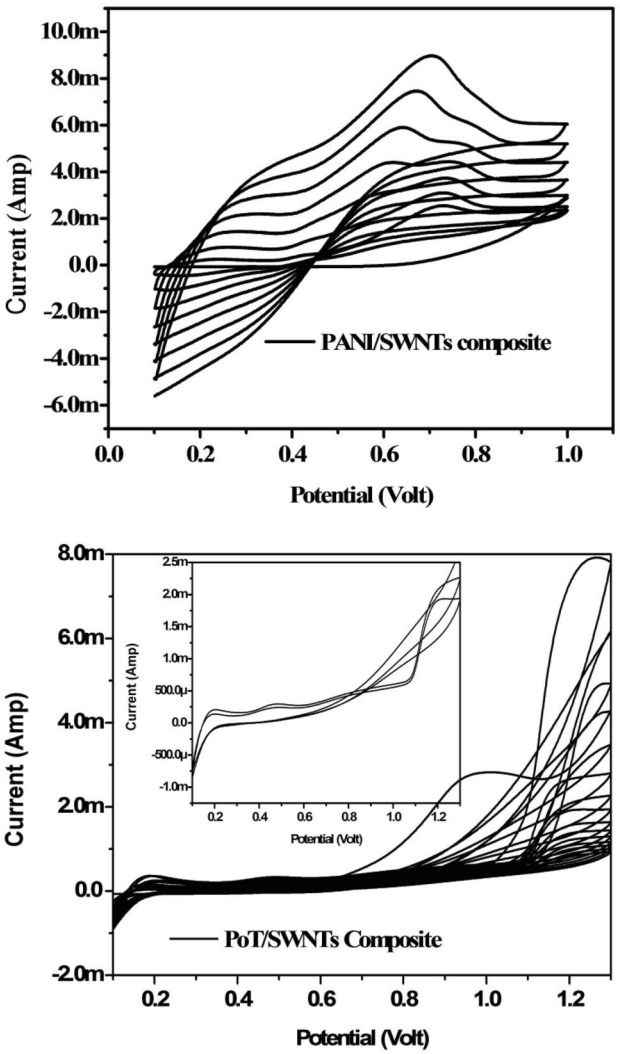

Fig. 1 Cyclic voltammogram recorded during electrochemical synthesis of PANI/SWNTs composite within potential window 0.1 to 1.0 V and PoT/SWNTs composite within potential window 0.1–1.2 V; with scan rate equal to 0.1 V per second, respectively

of functionalized SWNTs and amino groups [30]. Figure 2 depicts the formation of composite; PANI and PoT onto the surface of SWNTs, respectively. It was hypothesized that the OCPs will get deposited on the walls of SWNTs with the formation of tubular nature of both of the composites and the same was observed in the micrographs taken with the FESEM (corresponding micrographs of both composites are shown in Fig. 2).

3.2 SRIM analysis

The information of electronic energy loss (S_e) and nuclear energy loss (S_n) was taken from SRIM program. SRIM programme gives calculations/data of stopping powers, range, and straggling distributions for any ion at any

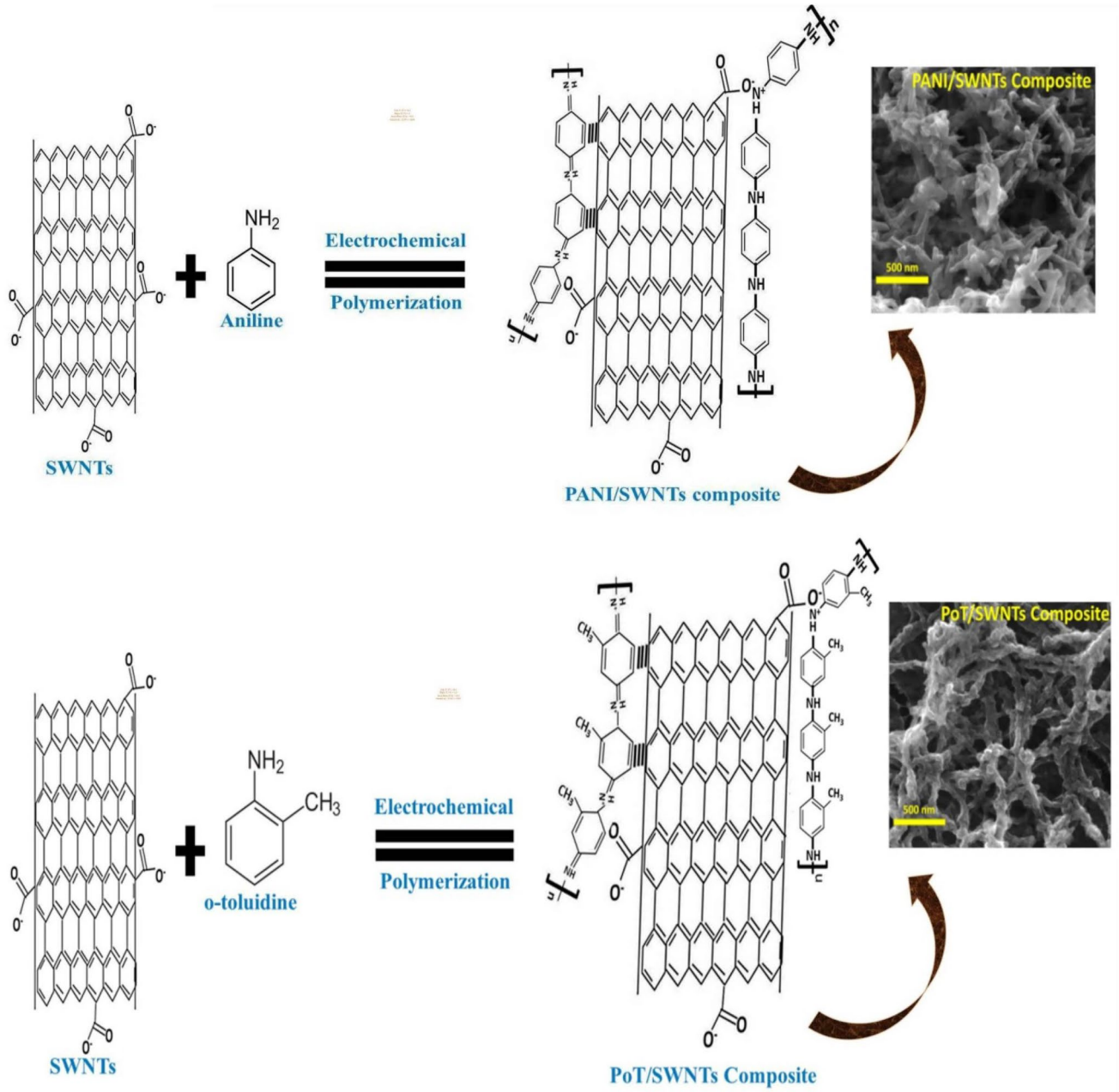

Fig. 2 Schematic of the electrochemical synthesis of PANI/ SWNTs composite and PoT/SWNTs composite (adjacent FESEM micrograph shows the respective composite)

energy in any elemental target. Figure 3 shows energy as a function of S_e and S_n for both composites. From Fig. 3a, b, it is clear that the electronic energy loss is greater than the nuclear energy loss. Therefore, it can be concluded that the electronic energy loss is dominant and is responsible for materials modifications. The physicochemical changes induced upon irradiation are well explained through Coulomb-explosion model and thermal-spike model. The Coulomb-explosion model explains that the intense ionization and excitation along the ion path leads to an unstable zone in which atoms are ejected into the non-excited part of the solid by Coulomb repulsion. In thermal-spike model, the energy deposited by the ion leads to a transient temperature increase and the cylindrical volume around the ion path melts due to electron–phonon coupling, which is subsequently quenched by thermal conduction [31]. Therefore, it can be claimed that SHI is useful technique in modifications of OCPs where the modifications are well explained through Coulomb-explosion model.

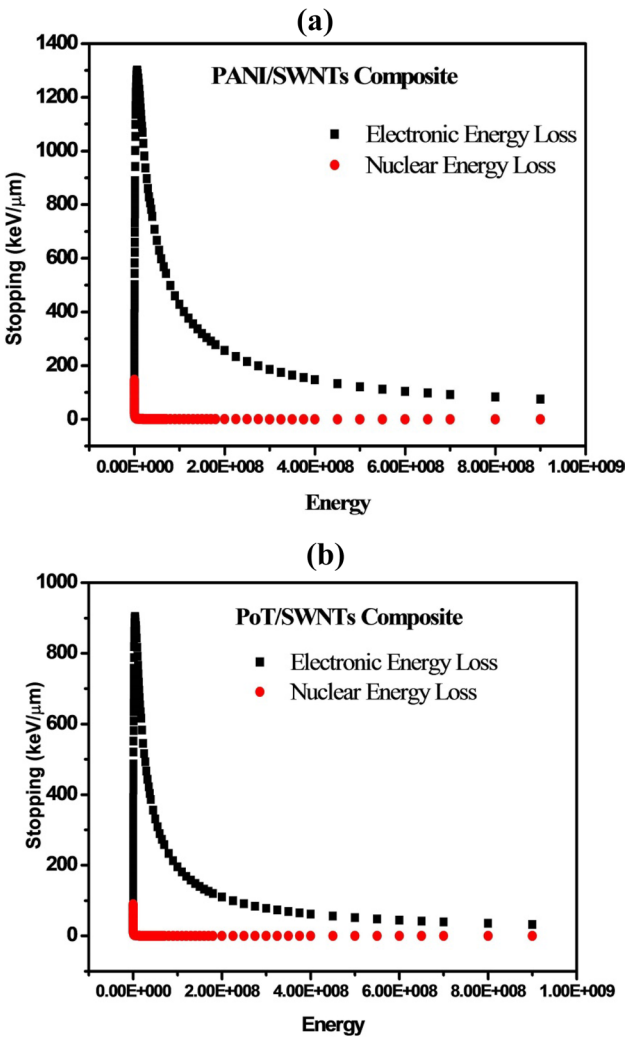

Fig. 3 Plot of electronic energy loss and nuclear energy loss versus energy evaluated form SRIM programme (version 2008.04) for PANI/SWNTs (**a**) and PoT/SWNTs composite (**b**)

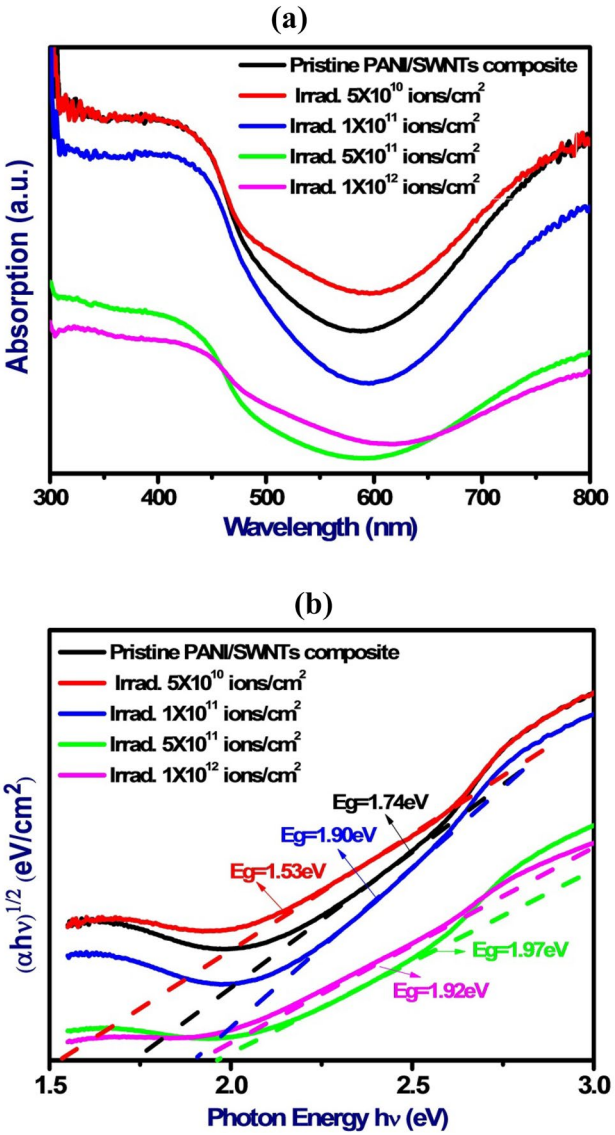

Fig. 4 **a** UV–Vis absorption spectra and **b** variation of $(\alpha h\nu)^{1/2}$ versus $h\nu$ of PANI/SWNTs before and after irradiation of 100 MeV oxygen ions with fluences 5×10^{10}, 1×10^{11}, 5×10^{11}, and 1×10^{12} ions/cm^2

3.3 Spectroscopic study

3.3.1 UV–Vis spectroscopy

The ultraviolet–visible (UV–Vis) absorption spectroscopy is widely used in the examination of optical properties of the materials. Figure 4a, b shows UV–Vis absorption spectra and band-gap variation obtained for composites of PANI/SWNTs before and after SHI irradiation. It was observed that upon SHI irradiation of oxygen ions results in average decrease in the absorption with increase in ion fluences. The absorption spectra were recorded in the range 300–800 nm at room temperature. The absorption spectra of pristine composite show absorption peaks at ~300–330 nm with extended tail. This indicates the π–π^* transition, which is assigned to the fact that there is transition from valence band to conduction band. The absorption at relatively low energy radiation indicates the charge transfer of benzoid and quinoid rings due to nonbonding free electrons. An increased absorption at ~725–800 nm is an indication of characteristic of an extended coil conformation and the π—polaron transition [32, 33]. The presence of these characteristic absorption bands indicates the interfacial interaction between SWNTs and PANI and hence revealed the formation of composite. The photonic absorptions of amorphous materials are found to obey Tauc relation of the form:

$$\alpha \mathrm{hn} = \mathrm{B}(\mathrm{hn} - E_g)^n,$$

where α is the absorption coefficient, hν is the photon energy, B is the band-gap tailing parameter, E_g is a characteristic

energy which is termed as optical bandgap, and n is the transition probability index, which has discrete values $n = 1/2$, 3/2, 2, and 3 for direct allowed, direct forbidden, indirect allowed, and indirect forbidden electronic transitions, respectively [34]. The determination of indirect transition energy gap the plot of $(\alpha h\nu)^{1/2}$ as a function of photon energy versus hν was plotted for PANI/SWNTs composite before and after irradiation, as shown in Fig. 4b. The linear portion of the curve revealed the indirect optical bandgap and intercept to the *x*-axis gives indirect transition energy gap. The values of the optical indirect transition energies were found to be equal to 1.74 eV for pristine and 1.53, 1.90, 1.97, and 1.92 eV after irradiation at respective fluences. It was observed that there is average increase in the indirect transition energy gap. It was observed that upon SHI irradiation of oxygen ions of different fluences on composite, there is average decrease in the absorption with increase in fluence rate. The increased bandgap reveals that there is defect creation due to SHI irradiation which has remarkable effect on conjugation of the electrons. It is attributed that there is chain scission and may be resulting into shortening of polymer chain matrix. Figure 5a, b shows UV–Vis absorption spectra and band-gap variation obtained for PoT/SWNTs before and after irradiation. The absorption spectra of PoT/SWNTs composite show absorption ~ 320 and ~ 720–800 nm which shows the π–π^* transition of benzoid rings, whereas peaks around ~ 420–450 nm can be attributed to polaron—π^* transition, respectively [35] before and after irradiation. It is observed that there is average increase in absorption with increase in irradiation fluence. From Tauc relation, the values were calculated for band energy which are equal to 2.62 eV for pristine composite and 2.62, 2.58, 2.62, and 2.69 eV respectively. It is observed that SHI irradiation of carbon ion beam has no measurable impact on band energy excluding fluences 1×10^{11} and 1×10^{12} ions/cm^2.

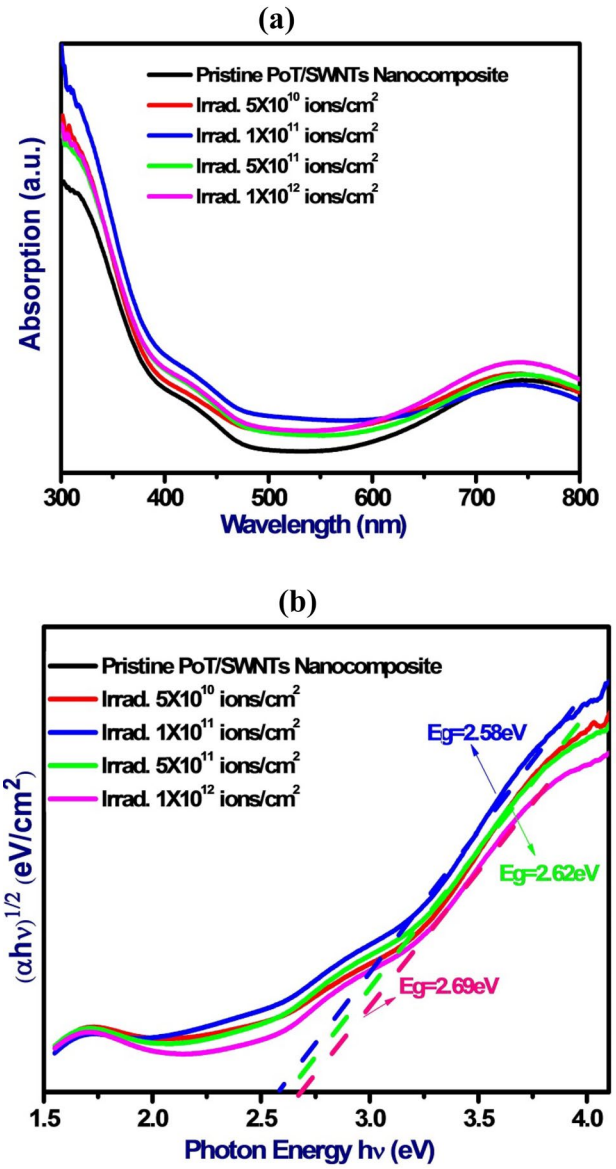

Fig. 5 **a** UV–Vis absorption spectra and **b** variation of $(\alpha h\nu)^{1/2}$ versus $h\nu$ of PoT/SWNTs before and after irradiation of 55 MeV carbon ions with fluences 5×10^{10}, 1×10^{11}, 5×10^{11}, and 1×10^{12} ions/cm^2

3.3.2 Fourier transformed infrared spectroscopy

Figure 6a, b shows the FT-IR transmission spectra of pristine and 100 MeV oxygen ion beam-irradiated PANI/SWNTs composite and 55 MeV carbon ion beam-irradiated PoT/SWNTs composite. FT-IR spectrum gives the information of IR active vibration modes present in the compound [36]. FT-IR spectra of PANI/SWNTs composite shown in Fig. 6a before and after irradiation show typical peaks at ~ 1500 and ~ 1600 cm^{-1} which are assigned with stretching of benzenoid and quinoid rings, respectively.

As observed in the spectra, peaks present for quinoid band at 1600 cm^{-1} are less intensive than benzenoid band at 1500 cm^{-1}. This indicates that the nature of the composite is having emeraldine salt, i.e., conductive form of polyaniline. It was observed that there is increase in the intensity of absorptions of benzenoid and quinoid band after SHI irradiation. This may be due to the formation of free radicals [30] as a result of irradiation.

The peaks, viz., ~1500 and 1600 cm^{-1}, are the characteristic peaks of nitrogen quinoid ring, 2300 cm^{-1} attributed to NH^+ stretching of the amine group, 2948 cm^{-1} attributed to N-H stretching mode of secondary amine [27], and 3405 cm^{-1} corresponds to the interstitial water and hydroxyl groups [37] present in PoT/SWNTs composite shown in Fig. 6b before and after irradiation of 55 MeV carbon ions. As observed in the both PANI/

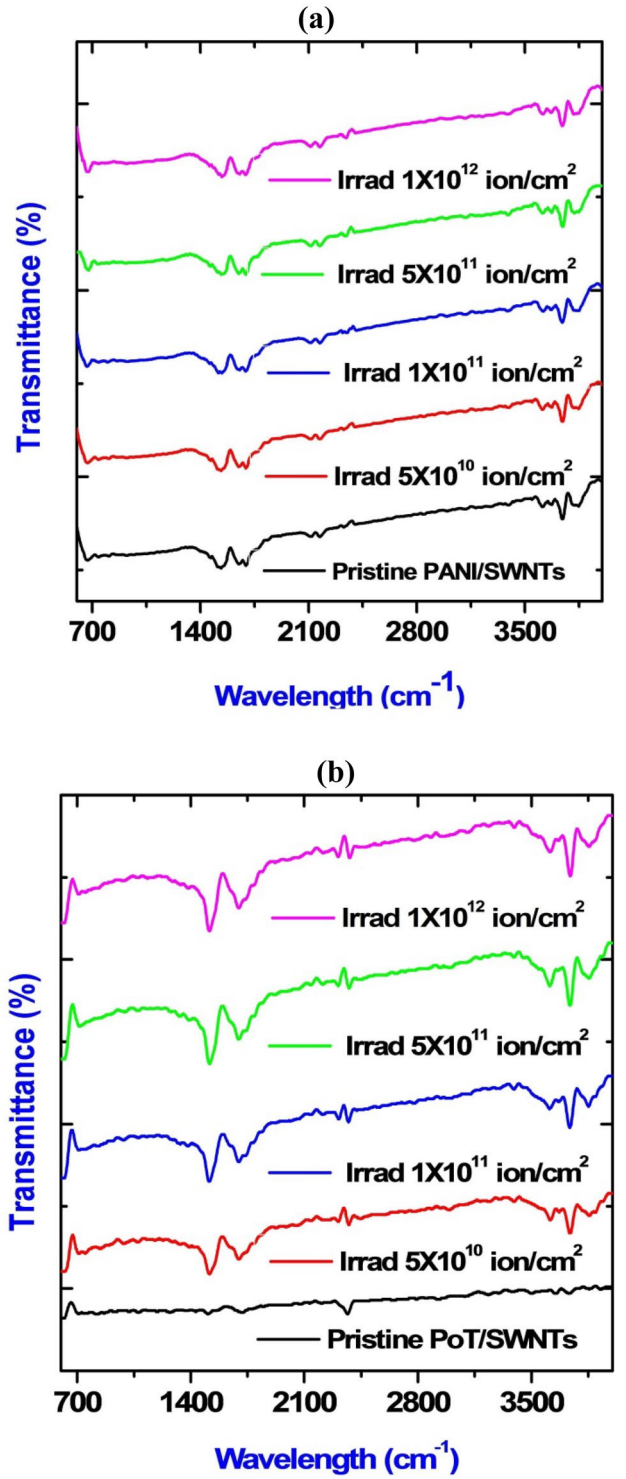

Fig. 6 FT-IR Transmission spectra of **a** PANI/SWNTs composite before and after 100 MeV oxygen ion irradiation and **b** PoT/SWNTs composite before and after 55 MeV carbon ion irradiation

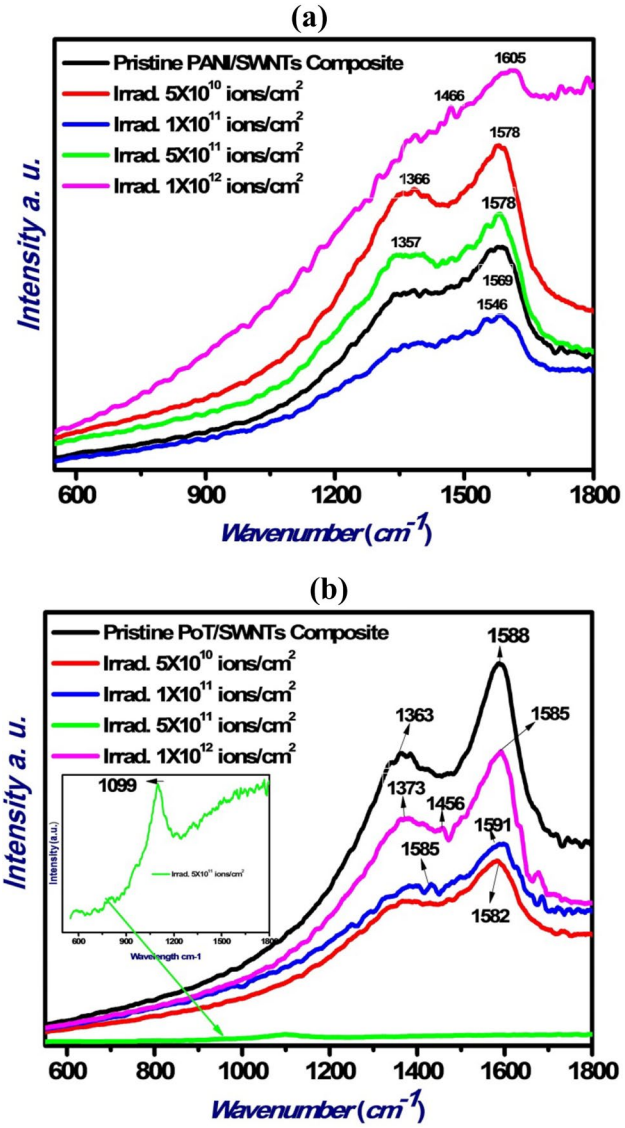

Fig. 7 Raman spectra of SHI-irradiated **a** PANI/SWNTs and **b** PoT/SWNTs composite before and after irradiation with oxygen ions (100 MeV) and carbon ions (55 MeV) with fluences 5×10^{10}, 1×10^{11}, 5×10^{11}, and 1×10^{12} ions/cm^2 respectively

SWNTs' composite and PoT/SWNTs' composite, there was substantial increase in the intensity of absorption for molecules as a result of SHI irradiation.

3.3.3 Raman spectroscopy

Raman spectroscopy is non-destructive tool which is sensitive to intra-molecular interaction, and, therefore, is able to

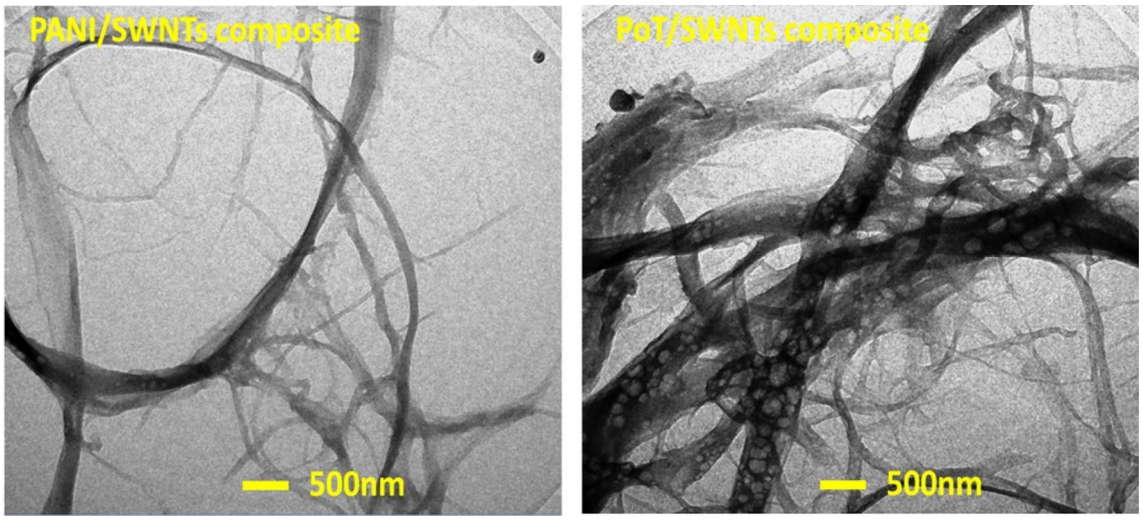

Fig. 8 Transmission electron microscopy images recorded for the confirmation of formation of composites PANI/SWNTs and PoT/SWNTs

give the information regarding overall chain structure regularity in case of semi-crystalline polymers [38]. Figure 7a, b shows Raman spectra of PANI/SWNTs and PoT/SWNTs composite before and after SHI irradiation. In the spectra of PANI/SWNTs and PoT/SWNTs composite, the band at ~ 1367 cm^{-1}, i.e., D band corresponds to the delocalized polaronic charge carriers indicating the conductive form of CP, ~ 1580 cm^{-1}, i.e., G band indicates C–C deformation bands of the benzenoid ring which are characteristics of the semiquinone rings [36, 39]. As observed for both the composites, the intensity of Raman active D band and G band decreases with increase in the fluence of SHI irradiation. This decrease in the Raman active modes directly indicates the amorphization of composite upon irradiation.

3.4 Morphological study

3.4.1 TEM

Figure 8 shows the TEM images of PANI/SWNTs and PoT/SWNTs composite, revealing the composite of both. It is apparent from the figures that both composites have formed different morphologies during polymerization, since the chemical structure of the monomer differs even though having same dopant and oxidative polymerization technique.

3.4.2 FESEM

Morphological investigations were carried out with the help of FESEM micrograph. Figures 9, 10 show the FESEM images of PANI/SWNTs and PoT/SWNTs composite before and after irradiation of oxygen and carbon ion, respectively. The FESEM images for both of PANI and PoT have shown the cable-like morphology of the composite formed with SWNTs. The planar structures of PANI and PoT adapted to the hexagonal surface lattice of SWNTs which leads to the strong interaction between PANI and SWNTs also PoT and SWNTs [30]. SWNTs functionalised with carboxyl group allow the growth of polymer chains from them [40]. It was observed that after irradiation fluences 5×10^{10}, 1×10^{11}, 5×10^{11}, and 1×10^{12} ions/cm^2, respectively, the composite structure remained persisted revealing its stability and adhesivity.

4 Conclusions

Composites of PANI/SWNTs and PoT/SWNTs were synthesized electrochemically and exposed to high-energy oxygen and carbon ion fluence ranges of 5×10^{10}–1×10^{12} ions/cm^2. The spectroscopic and morphological investigations showed changes in the composites after SHI irradiation. The bandgap calculated with UV–Vis spectra using Tauc plot shows the significant changes in the band-gap values upon irradiation. From FT-IR spectral bands, it was concluded that the synthesized form of composite is emeraldine salt which is having conductivity in semiconducting regime and is consistent with the results of band-gap values. The Raman spectroscopic results show the broadening of bands upon irradiation showing the amorphization which can result

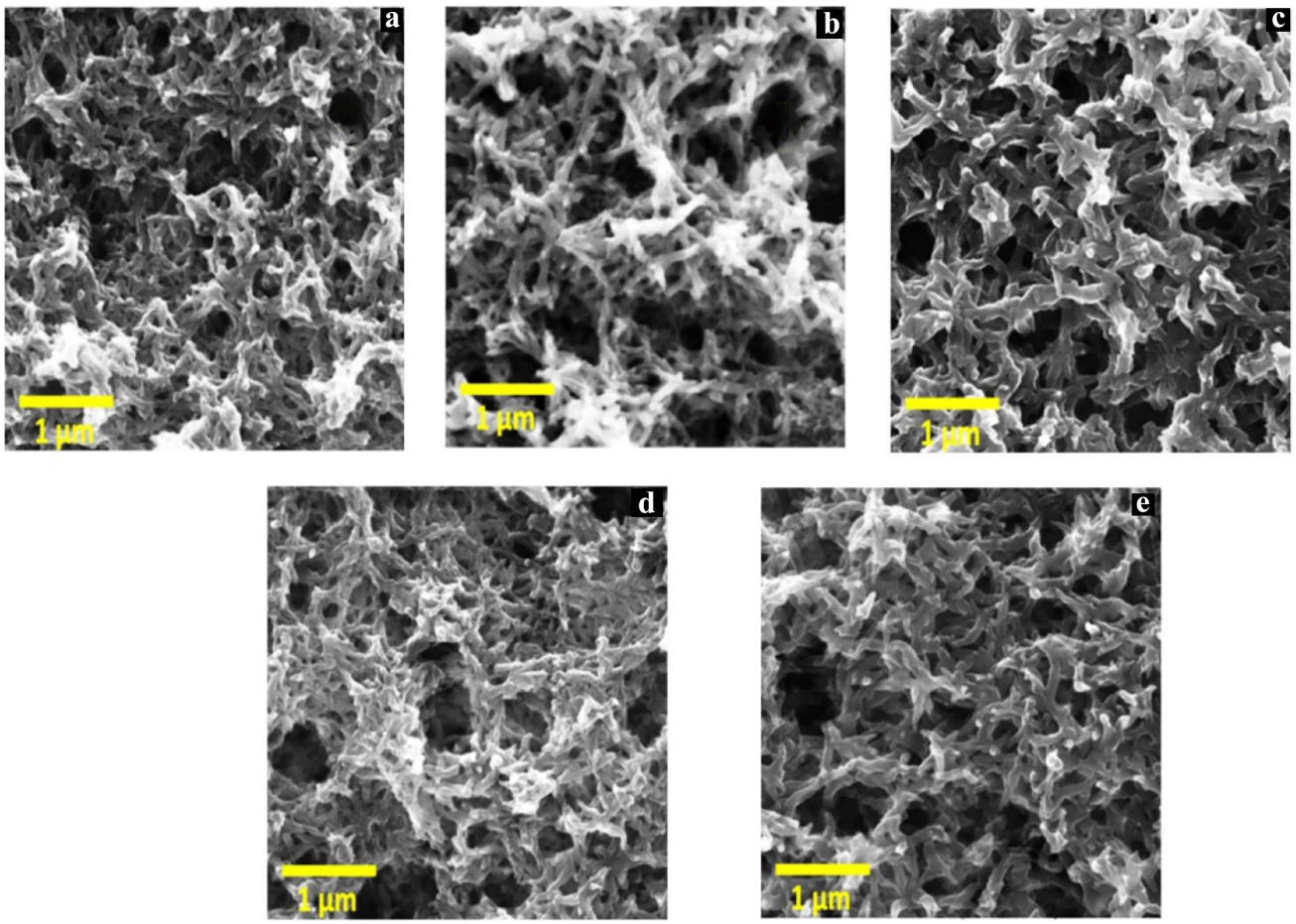

Fig. 9 FESEM images of SHI-irradiated PANI/SWNTs composite before (**a**) and after irradiation of oxygen ions at different fluences (**b** 5×10^{10} ions/cm^2) (**c** 1×10^{11} ions/cm^2) (**d** 5×10^{11} ions/cm^2) (**e** 1×10^{12} ions/cm^2)

into the densification and porous nature of composite which is well elaborated in morphological investigations, i.e., FESEM micrographs. All above observations revealed that the SHI irradiation is suitable tool for tailoring the properties of composites PANI/SWNTs and PoT/SWNTs which can be applied in the field of chemical sensors.

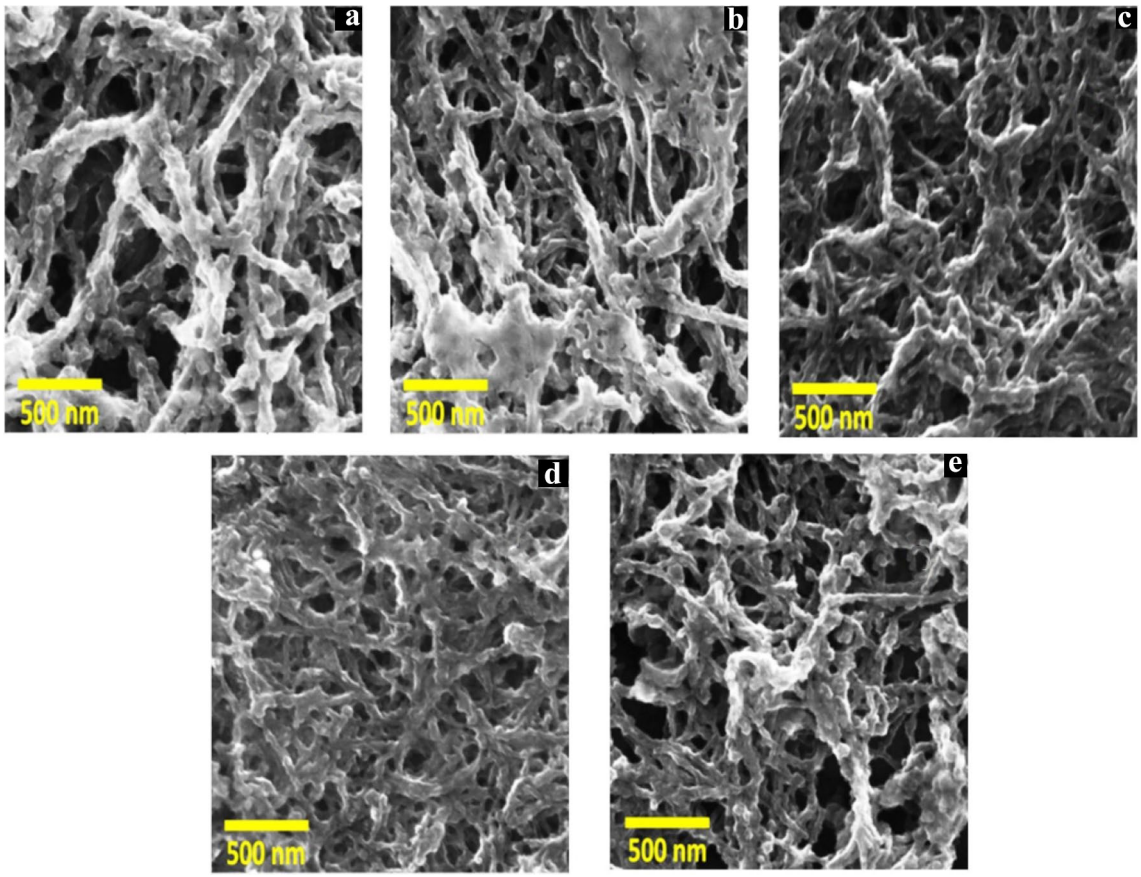

Fig. 10 FESEM images of SHI-irradiated PoT/SWNTs composite before (**a**) and after irradiation of oxygen ions at different fluences (**b** 5×10^{10} ions/cm^2) (**c** 1×10^{11} ions/cm^2) (**d** 5×10^{11} ions/cm^2) (**e** 1×10^{12} ions/cm^2)

Acknowledgements Authors extend their sincere thanks to Inter University Accelerator Centre (IUAC), New Delhi, India (UFR no. 55305) and DST, SERB, New Delhi (Project no.: SB/ EMEQ-042/2013), Rashtria Uchachatar Shiksha Abhiyan (RUSA), Government of Maharashtra, UGC-DAE-CSR–RRCAT Indore (Project no.: CSR-IC-BL66/CRS-183/2016-17/847), UGC-SAP Programme (F.530/16/DRS-I/2016(SAP-II) Dt. 16-04-2016) for providing financial support.

References

1. N. Hyeonseok Yoon, Nanomaterials, 3, 524–549 (2013)
2. M.D. Shirsat, M.A. Bangar, M.A. Deshusses, N.V. Myung, A. Mulchandani, Appl. Phys. Lett. **94**, 083502 (2009)
3. K. Datta, P. Ghosh, M.A. More, M.D. Shirsat, A. Mulchandani, J Phys D, https://doi.org/10.1088/0022-3727/45/35/355305
4. A. Sumedh Gaikwad, Y.-H. Rushi, M. Kim, H. Deshmukh, G. Patil, M.D. Bodkhe, A. Shirsat, P. Koinkar, A. Mulchandani, Mod. Phys. Lett. B **29**, 1540046 (2015)
5. J. Janata, M. Josowicz, Nat. Mater. **2**, 19–24 (2003)
6. U. Lange, N.V. Roznyatovskaya, V.M. Mirsky, Anal. Chim. Acta **614**, 1–26 (2008)
7. Z.F. Li, F.D. Blum, M.F. Bertino, C.S. Kim, Sens. Actuators B. **183**, 419–427 (2013)
8. T. Rajesh, D. Ahuja, Kumar, Sens. Actuators B. **136**, 275–286 (2009)
9. P. Kar, A. Choudhury, Sens. Actuators B. **183**, 25–33 (2013)
10. J. Xu, P. Yao, X. Li, F. He, Mater. Sci. Eng., B **151**, 210–219 (2008)
11. P. Pieta, F. D'Souza, I. Obraztsov, W. Kutner, ECS J. Solid State Sci. Technol. **2**(10), M3120-M3134 (2013)
12. S. Bose, T. Kuila, A.K. Mishra, R. Rajasekar, N.H. Kim, J.H. Lee. J. Mater. Chem. **22**, 767 (2012)
13. C. Peng, S. Zhang, D. Jewell, Z. George, Chen, Prog. Nat. Sci. **18**, 777–788 (2008)
14. J. Yang, Y. Liu, S. Liu, L. Li, C. Zhang, T. Liu. https://doi.org/10.1039/c6qm00150e
15. A.M.P. Hussain, A. Kumar, F. Singh, D.K. Avasthi, J. Phys. D: Appl. Phys. **39**, 750–755 (2006)
16. P. Ghosh, K. Datta, A. Mulchandani, R.G. Sonkawade, K. Asokan, D.M. Shirsat, Smart Mater. Struct. **22**, 035004 (2013) (8 pp)
17. S.B. Kadam, K. Datta, P. Ghosh, A.B. Kadam, P.W. Khirade, V. Kumar, R.G. Sonkawade, A.B. Gambhire, M.K. Lande, M.D. Shirsat, Appl Phys A (2010)
18. D.K. Avasthi, Curr. Sci. **78**(11), 10 (2000)
19. A.M.P. Hussain, A. Kumar, Eur. Phys. J. Appl. Phys. **36**, 105–109 (2006)
20. A.M.P. Hussain, D. Saikia, F. Singh, D.K. Avasthi, A. Kumar, Nuclear Instrum. Methods Phys. Res. B **240**, 834–841 (2005)
21. A. Amarjeet Kaur, D.K. Dhillon, Avasthi, J. Appl. Phys. **106**, 073715 (2009)
22. C. Downs, J. Nugent, P.M. Ajayan, D.J. Duquette, K.S. Santhanam, Adv. Mater. 11(12), 1028–1031 (1999)

23. A.B. Kaiser, Rep. Prog. Phys. **64**, 1–49 (2001)
24. M.A. Deshmukh, H.K. Patil, G.A. Bodkhe, M. Yasuzawa, P. Koinkar, A. Ramanavicius, S. Pandey, M. Shirsat, Colloids Surf. A **537**, 303–309
25. M.A. Deshmukh, H.K. Patil, M.D. Shirsat, A. Ramanavicius, AIP Conference proceedings 1832 (1), p. 050084
26. M. Hasik, A. Drelinkiewicz, E. Wenda, C. Paluszkicz, S. Quillard, J. Mol. Struct. **596**, 89–99 (2001)
27. V.A. Anand Kumar, S. Kumar, M. Husain, Int. J. Polym. Anal. Charact. **16**, 298–306 (2011)
28. S.P. Surwade, S.R. Agnihotra, V. Dua, S.K. Manohar, Sens. Actuators B **143**, 454–457 (2009)
29. A. Arratia, H. Gomez, R. Schrebler, R. Cordova, M.A. del Valle, J Electr Chem **377**(1), 75–83 (1994)
30. K. Harshada, H.K. Patil, Megha, M.A. Deshmukh, S.D. Gaikwad, G.A. Bodkhe, K. Asokan, M.D. Shirsat, M. Yasuzawa, P. Koinkar, D. Mahendra, Radiat. Phys. Chem. **130**, 47–51 (2017)
31. A. Kumar, S. Banerjee, P. Jyoti, B.K. Saikia, Konwar, Nanotechnology 21 (2010) (8 pp) 175102
32. V. Milind, A.K. Kulkarni, Viswanath, Eur. Polymer J. **40**, 379–384 (2004)
33. R.K. Agrawall, V. Meriga, R. Paul, A.K. Chakraborty, A.K. Mitra, eXPRESS Polym. Lett. **10**(9), 780–787 (2016)
34. S.M. Pethe, S.B Kondawar, Adv. Mat. Lett **5**(12), 728–733 (2014)
35. S. Ding, X. Lu, J. Zheng, W. Zhang, Mater. Sci. Eng. B **135**, 10–14 (2006)
36. A. Kumar, S. Banerjee, Adv. Mat. Lett **4**(6), 433–437 (2013)
37. S. Dhanavel, E.A.K. Nivethaa, D. Sangamithirai, V. Narayanan, A. Stephen, Int. J. Innov. Res. Sci. Eng. (ISSN 2347-3207, online)
38. A. Crawford, E. Silva, K. York, C. Li, Raman spectroscopy: a comprehensive review. https://www.academia.edu/1131363/Raman_Spectroscopy_A_Comprehensive_Review
39. J. Xu, P. Yao, X.L.F. He, Mater. Sci. Eng. B **151**, 210–219 (2008)
40. M.A. Bavio, G.G. Acosta, T. Kessler, J. Power Sour. **245**, 475e481 (2014)